Original Article

Meniscus regeneration with injectable Pluronic/PMMA-reinforced fibrin hydrogels in a rabbit segmental meniscectomy model

Journal of Tissue Engineering
Volume 12: 1–14

DOI: 10.1177/20417314211050141
journals.sagepub.com/home/tej
SAGE

Young-Hyeon An[1,2*], Jin-A Kim[3,4*], Hyun-Gu Yim[1], Woo-Jung Han[4,5], Yong-Beom Park[6], Hyun Jin Park[4,5], Man Young Kim[5], Jaewon Jang[5], Racheal H. Koh[1], Su-Hwan Kim[7,8], Nathaniel S. Hwang[1,2,7] and Chul-Won Ha[3,4,5]

Abstract

Injectable hydrogel systems are a facile approach to apply to the damaged meniscus in a minimally invasive way. We herein developed a clinically applicable and injectable semi-interpenetrated network (semi-IPN) hydrogel system based on fibrin (Fb), reinforced with Pluronic F127 (F127) and polymethyl methacrylate (PMMA), to improve the intrinsic weak mechanical properties. Through the dual-syringe device system, the hydrogel could form a gel state within about 50 s, and the increment of compressive modulus of Fb hydrogels was achieved by adding F127 from 3.0% (72.0 ± 4.3 kPa) to 10.0% (156.0 ± 9.8 kPa). The shear modulus was enhanced by adding PMMA microbeads (26.0 ± 1.1 kPa), which was higher than Fb (13.5 ± 0.5 kPa) and Fb/F127 (21.7 ± 0.8 kPa). Moreover, the addition of F127 and PMMA also delayed the rate of enzymatic biodegradation of Fb hydrogel. Finally, we confirmed that both Fb/F127 and Fb/F127/PMMA hydrogels showed accelerated tissue repair in the in vivo segmental defect of the rabbit meniscus model. In addition, the histological analysis showed that the quality of the regenerated tissues healed by Fb/F127 was particularly comparable to that of healthy tissue. The biomechanical strength of the regenerated tissues of Fb/F127 (3.50 ± 0.35 MPa) and Fb/F127/PMMA (3.59 ± 0.89 MPa) was much higher than that of Fb (0.82 ± 0.05 MPa) but inferior to that of healthy tissue (6.63 ± 1.12 MPa). These results suggest that the reinforcement of Fb hydrogel using FDA-approved synthetic biomaterials has great potential to be used clinically.

Keywords

injectable hydrogel, biomaterials, meniscus repair, rabbit meniscectomy, translational research

Date received: 13 June 2021; accepted: 15 September 2021

[1]School of Chemical and Biological Engineering, Institute of Chemical Processes, Seoul National University, Seoul, Republic of Korea
[2]Bio-MAX/N-Bio Institute, Institute of Bioengineering, Seoul National University, Seoul, Republic of Korea
[3]Department of Health Sciences and Technology, SAIHST, Sungkyunkwan University, Seoul, Republic of Korea
[4]Stem Cell & Regenerative Medicine Research Institute, Samsung Medical Center, Seoul, Republic of Korea
[5]Department of Orthopedic Surgery, Samsung Medical Center, Sungkyunkwan University School of Medicine, Seoul, Republic of Korea
[6]Department of Orthopedic Surgery, Chung-Ang University Hospital, Chung-Ang University College of Medicine, Seoul, Republic of Korea
[7]Interdisciplinary Program in Bioengineering, Seoul National University, Seoul, Republic of Korea
[8]Department of Chemical Engineering (BK21 FOUR), Dong-A University, Busan, Republic of Korea

*These authors contributed equally to this work.

Corresponding authors:
Chul-Won Ha, Department of Orthopedic Surgery, Samsung Medical Center, Sungkyunkwan University School of Medicine, 81 Irwon-ro, Gangnam-gu, Seoul 06351, Republic of Korea.
Email: chulwon.ha@gmail.com

Nathaniel S Hwang, School of Chemical and Biological Engineering, Institute of Chemical Processes, Seoul National University, 1 Gwanak-gi Gwanak-Ro, Building 302 Room 913, Seoul 08826, Republic of Korea.
Email: nshwang@snu.ac.kr

Introduction

The spontaneous regeneration of the damaged meniscus is limited. The meniscus is fibrous cartilage that absorbs shock and provides stability to the knee joint and is known to be constantly damaged or depleted by various internal or external factors, such as age-related degeneration and sports-related injuries.[1] Meniscal allograft,[2–4] polyurethane-based meniscal implants (Actifit™, Orteq Ltd., London, UK)[5–8] and collagen-based meniscal implants (CMI™, ReGen Biologics, USA)[9–12] are currently being used in clinical practice for the treatment of damaged meniscal chondrocytes. In meniscus implantation procedures, it is essential to reconstruct a continuous meniscal wall, essentially in the late compartment, with strong posterior-anterior roots and a stable knee joint or stabilized knee joint, and the lower extremity should also be well aligned.[13,14]

Although these meniscal implants have been reported to be successful considering the intermediate results among surgical methods,[12,15] it is still challenging to regenerate the damaged meniscal cartilage using non-surgical methods. The injection-based strategy has the advantages of simple operation procedures and avoiding patient discomfort. Non-surgical strategies using an injection of cells or hydrogels have been reported[16–22]; however, most of the injectable systems were comprised of biomaterials that have not been yet approved clinically; also, they had weak mechanical stress to effectively relieve the load-bearing stresses applying to the meniscus. Therefore, it is necessary to develop mechanically stable and highly bioactive biomaterials for translational research using FDA-approved biomaterials. Fibrin (Fb) is a naturally-derived biopolymer that can be polymerized by thrombin action. Albeit it has been used as a bio-glue or bio-adhesive, the poor mechanical property and rapid biodegradability limit its applications to the load-bearing implants[23]; therefore, incorporation of other biomaterials, such as polyethylene oxide (PEO), into the Fb network boosts their mechanical properties and broaden its biomedical applications.[24–26]

Among the synthetic polymers, Pluronic® F-127 (F127) is a commercially available synthetic polymer exhibiting little toxicity and thermo-reversible property. Behaving as a sol at or below ambient temperature and transits into a gel at around body temperature, F127 has been used as a drug carrier, injectable hydrogels, etc.[27,28] We have herein developed an injectable hydrogel system using a combination of Fb and F127 for treating segmental defects of the meniscus with a non-surgical method. We hypothesized that F127 would reinforce the mechanical property of the Fb hydrogel via forming a semi-interpenetrated polymer (semi-IPN) network. In addition, poly(methyl methacrylate) (PMMA) is a synthetic and thermoplastic biomaterial that can strengthen the mechanical property of biomedical composite materials.[29–31] In our study, we incorporated commercially available PMMA microbeads in the Fb/F127 hydrogel to reinforce the mechanical properties of hydrogels further. We investigated whether the mechanical reinforcement via PMMA microbeads would allow effective regeneration of the damaged meniscus tissues. The injectable and composite hydrogel system would provide insights into translational research and therapeutic options using clinically available biomaterials.

Materials and methods

Materials

Fibrinogen from bovine plasma (F8630), Pluronic® F-127 (F127, P2443), aprotinin from bovine lung (A1153), and calcium chloride ($CaCl_2$) were purchased from Sigma-Aldrich. Thrombin lyophilized powder was obtained from Reyon Pharmaceutical Co., Ltd. (Republic of Korea). Poly(methyl methacrylate) (PMMA) was purchased from Polysciences (04553-500, 200 μm atactic polymer beads).

Fabrication of injectable Fb/F127/PMMA hydrogel

The injectable hydrogel system was implemented using a dual-syringe, which could separate the fibrinogen and thrombin parts with modification of the previous study.[24] In fibrinogen part, fibrinogen (100 mg/mL) was dissolved in saline (0.9% NaCl) with adding the aprotinin (0.5 mg/mL). In the thrombin part, the thrombin was dissolved at 2500 U/mL, followed by adding F127 (3.0%, 7.0%, and 10.0%, w/v) and PMMA (3.0% and 6.0%, w/v) with adding $CaCl_2$ (50 mg/mL). Each part was extruded through the dual-syringe needle, where in situ gelation process occurred.

Scanning electron microscopy (SEM)

The microstructure of the hydrogels was observed by Field Emission Scanning Electron Microscopy (FE-SEM, JSM 6700F, JEOL, Japan). The hydrogels were fixed by 4% paraformaldehyde and washed with phosphate buffer, followed by lyophilized. The cross-sectional plane of the dried hydrogel was observed.

Swelling ratio

The swelling ratio of the hydrogels was measured according to the following equation:

$$\text{Swelling ratio} = \frac{Ws - Wd}{Wd} \text{ x } 100 \ (\%)$$

where W_s and W_d represent the weights of the swollen hydrogel and the dried hydrogel, respectively.

Compressive test

The compressive strength of the hydrogel was estimated using the universal testing machine (EZ-Test, Doing-il SHIMADZU Crop.). The hydrogel was fabricated in a cylindrical shape with a diameter of 8 mm and a height of 4 mm. The samples were pressed by the 8 mm-diameter load cell, and the compressive modulus was calculated from the stress-strain curve, where the strain region was about 5% to 15%.

Rheological test

The rheological properties of the hydrogel were analyzed using a rheometer (MCR 302, Anton-Paar, Austria). The hydrogels were prepared with 8 mm in diameter and 2 mm in height. To investigate the gelation time at 37°C, the shear storage modulus (G') and loss modulus (G'') were measured depending on the time, where the strain and frequency were fixed at 5% and 10^1 Hz. The shear-mediated breakage was analyzed using a strain-sweep test by altering the strain from 0.1% to 500%. In a frequency-sweep test, the oscillatory frequency increased from 10^{-1} to 10^2 Hz, and both the G' and G'' were measured at 16 points.

Cytotoxicity test

To determine the cytotoxicity of the hydrogel component, the Live/Dead assay was performed after encapsulating the fibrochondrocytes within the hydrogel. Fibrochondrocytes were isolated from the New Zealand white rabbit, as previously described.[32] The cells were maintained in DMEM/F-12 (Gibco) supplemented with 10% fetal bovine serum and 100 U/mL Pen-strep. The cells were suspended in the fibrinogen solution with 1×10^5 cells mL^{-1} and extruded through the dual-syringe system while mixing with the thrombin solution. The cytotoxicity was evaluated until 7 days through the Live/Dead assay, which treated the encapsulated cells with calcein-AM (Live, green) and ethidium homodimer-1 (Dead, red). The fluorescent images were obtained using confocal laser scanning microscopy (CLSM).

In vitro degradation test

The in vitro degradative behavior of the hydrogels was estimated. The hydrogels were fabricated 8 mm in diameter and 4 mm in height and soaked in the 0.00125% trypsin-EDTA solution. At each time point, the weight of the hydrogels was measured and compared to the initial weight.

Meniscectomy and hydrogels injection

For the in vivo test, 78 healthy New Zealand white male rabbits (weight 3.0–3.5 kg) were used. All animals were obtained 1 week before the experiment and grew in the same environment. All procedures and experimental plans have been reviewed and approved by the Institutional Animal Care and Use Committee of our institution (Samsung Medical Center, Seoul. South Korea, approval 20130808002). This study followed the National Institutes of Health guidelines for the care and use of laboratory animals.

The rabbit was administered chlorine hydrate and was under general anesthesia. Then the patellar ligament and joint capsule were released through longitudinal incisions inside both knees to expose the meniscus.[33–35] By removing about 60% of the medial meniscus, including the central portion, was excised from the anterior portion, meniscus defects occurred, and the wound closed in layers. After 1 week, Fb, Fb/F127, and Fb/F127/PMMA hydrogels were injected into the area of the missing meniscus without a skin incision. Specifically, a needle was inserted into the joint space between the femur and tibia. Touch the tibial plateau of the front knee with the tip of the needle to check the position where the meniscus was excised. Self-molding was carried out by injecting hydrogel at the same rate from back to front to the identified ablation site. Meniscal defects in the meniscus were not treated as control ($n = 8$ for 4, 8, and 12 weeks). Fb, Fb/F127, and Fb/F127/PMMA hydrogels were injected into both knees to evaluate compression modulus at 12 weeks ($n = 3$ for 12 weeks). All rabbits were able to move their knee joints freely without restriction within the cage, and the clinical symptom was observed daily. Meniscus regeneration was assessed by sacrificing animals 4, 8, and 12 weeks after injection (Table 1). Due to abnormal clinical findings, animals were not excluded.

Gross observation

An arthrotomy was done to examine the joints, looking for abnormal results suggesting rejection or infection, such as severe inflammation or extensive fibrosis. Each knee was separated by a sharp resection of the femoral attachment of the femur, collateral, and cruciate ligaments. The medial meniscus was carefully separated from the femur and tibia at 4, 8, and 12 weeks after injection. The femur and tibia condyles were stained with ink to confirm cartilage degeneration 12 weeks after injection.[36] Macroscopic pictures were taken using Olympus MVX 10 (Olympus, Tokyo, Japan). Quantification of regenerated crescent size was using the software Image J (National Institutes of Health, Bethesda, Maryland).[37]

Histological analysis

All samples were fixed in 4% paraformaldehyde, decalcified, and embedded in paraffin. The specimen was then cut

Table 1. Study design of in vivo rabbit meniscectomy model.

Groups	Experiment		Study period	Number of animals
	Right	Left		
Group 1	Meniscectomy only	Meniscectomy + Fb	4, 8, and 12 weeks	27
Group 2	Meniscectomy + Fb	Meniscectomy + Fb/F127	4, 8, and 12 weeks	24
Group 3	Meniscectomy + Fb/F127	Meniscectomy + Fb/F127/PMMA	4, 8, and 12 weeks	27

into slices 5 μm thick in the radial direction for the meniscus. For histological analysis, hematoxylin and eosin (H&E) staining, Safranin-O staining, immunohistochemical staining for type I and II collagen were performed according to the manual provided by the manufacturer.[38] Images of the stained area were recorded using an optical microscope (Model Nikon Eclipse 600; Nikon Corp., Tokyo, Japan) equipped with a digital camera (Nikon DXM1200F).

Based on a conventional quantitative scoring system, three-dimensional recoverable meniscal tissue quality was assessed as previously reported.[39,40] Regeneration tissue was assessed using original semi-quantitative scoring using three observers blind to treatment. The evaluation points can be divided into three as follows: (1) Evaluate whether the repair tissue is attached to the normal meniscus tissue surrounded by the repair tissue; (2) the presence of fibrochondrocytes; and (3) the ability to stain with Safranin-O. The total achievable score is 6 points and 2 points for each category. Points were calculated statistically and histologically for each sample.

Biomechanical evaluation

The mechanical compression properties of the meniscus were carried out using an Instron tension/compression system with fast track software (Model 5543; Instron) as described above ($n=3$ for the treated group and $n=3$ for the control group).[33] Samples were collected from the central region of the regenerated meniscus at 12 weeks post-treatment. The meniscus was pierced from perpendicular direction to horizontal plane by using a 4-mm biopsy punch, followed by processing the circumferential planes. The samples were placed in PBS for 3–4 h at room temperature to equilibrate before testing. For the compression test, use a humidifier during the compression test to keep it moist. The compression force was applied using a 1 mm diameter cylindrical indenter equipped with a maximum 10 N load cell, and the crosshead speed was about 0.06 mm/min. To determine the unconstrained equilibrium coefficient, a step displacement (15% strain) was applied, and the compressive force was monitored until equilibrium was reached.

Statistical analysis

All quantitative data sets are expressed as mean-SD. The student's t-test was performed to assess whether there were statistically significant differences between the data sets. Pre-power calculations were performed using mean and standard deviation assumptions based on previously published data on the quality of the meniscus tissue.[22] Based on the a priori power analysis, a sample size of eight rabbits at each endpoint was selected to achieve 90% power to detect a three-point difference between MS and control mean tissue quality scores. The Wilcoxon sign grading test was used to compare the quantity and quality of tissue recovered from MS and to control meniscus defects at each of the three endpoints. A p-value <0.05 was considered statistically significant.

Results

Hydrogel fabrication and modulation of mechanical properties

The mechanical behavior of fibrin-based hydrogel can be modulated on the amount of fibrinogen, thrombin, and other additive molecules.[41] We herein used two synthetic polymers, Pluronic® F-127 (F127) and poly(methyl methacrylate) (PMMA), to compensate for the innate poor mechanical property of the fibrin (Fb) by forming the interpenetrated network (IPN) structure. We have optimized the thrombin concentration (1,50 U mL^{-1}) for in situ gelations of the Fb and assessed both compressive and shear modulus of the hydrogels by varying the concentration of polymers. The compressive modulus of hydrogels was increased with higher F127 contents from 3.0%, 7.0%, and 10.0%, which had 72.0 ± 4.3, 122.0 ± 9.6, and 156.0 ± 9.8 kPa, respectively (Figure 1(a)). Meanwhile, there was no significant increment of compressive strength despite the increase of PMMA contents (Figure 1(b)), and we decided to use Fb hydrogel with the concentration of F127 at 10.0% and PMMA at 6.0% in the following experiments.

In order to demonstrate the in situ gelation profile, we observed the gelation time after injection by using time

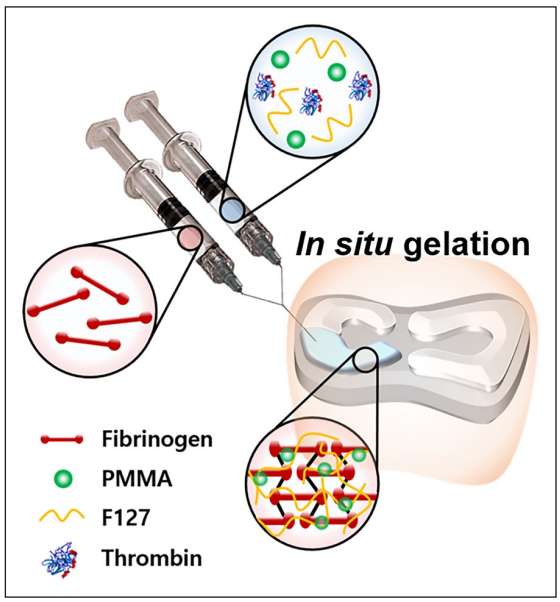

Figure 1. Scheme of the gelation process of Fb/F127/PMMA hydrogel through the dual-syringe device and filling the meniscal defect region. The semi-IPN hydrogel is formed immediately once the fibrinogen is mingled with the thrombin, where the F127 polymers are entangled with the Fb networks.

sweep mode. All of the hydrogels displayed elastic behavior (G'>G'') within 30 s at 37℃, and the shear modulus was gradually increased (Figure 1(c)). Furthermore, the shear-mediated breakage was investigated by strain sweep mode. The Fb and Fb/F127 groups lost elastic behaviors at a strain of about 156% and 190%, respectively; however, Fb/F127 + PMMA group had the highest resistance to shear-mediated breakage showing the gel breakage point at about 400% (Figure 1(d)). We finally measured the shear modulus of hydrogels after 24 h post-gelation process. The Fb/F127+PMMA had the highest shear modulus of 26.0 ± 1.1 kPa, and Fb/F127 had 21.7 ± 0.8 kPa, while Fb displayed 13.5 ± 0.5 kPa (Figure 1(e)). As a result, both F127 and PMMA could effectively improve the shear modulus of Fb.

The microstructure and swelling ratio of the hydrogels

We observed the microstructure of hydrogels using scanning electron microscopy (SEM). All of the hydrogels had interconnected porous structures attributed to the fibrin networks (Figure 2(a)). In the magnified images, Fb/F127 showed the polymer branches of F127 that protruded from the fibrin wall, which revealed that the hydrogel formed a semi-IPN structure. Furthermore, we could observe that PMMA microbeads incorporated within the hydrogel pores as described in Figure 3.

The swelling ratio of Fb (1217 ± 161.9) and Fb/F127 (1269 ± 39.7) was not much different, whereas that of Fb/F127/PMMA (567.6 ± 17.3) was far more diminished since PMMA microbeads occupied the void spaces in the hydrogel (Figure 2(b)).

In vitro cytotoxicity and degradative profile

The biological properties of the hydrogels, such as cytotoxicity and biodegradation behavior, are essential for providing a favorable environment for host cells to regenerate the damaged tissues.[42] We first investigated in vitro cytotoxicity of the hydrogels encapsulating the fibrochondrocytes via Live/Dead assay (Figure 4(a)). Until 7 days, all of the hydrogels displayed little cytotoxicity, with the cell viability over 95% (Figure 4(b)).

Next, we confirmed that both F127 and PMMA would inhibit the degradation of Fb, which then supported the integration of the hydrogel and the host tissues. We could observe the hydrogel structure of Fb was loosen at day 4, while both Fb/F127 and Fb/F127/PMMA hydrogels relatively retained the structural stability (Figure 5(a)). By measuring the mass ratio of the hydrogels, we could confirm that the degradation rate became remarkably slower in Fb/F127 and Fb/F127/PMMA than in Fb only group, and the resistance to degradation increased by adding PMMA to Fb/F127 (Figure 5(b)).

In vivo tissue regeneration of rabbit meniscus

We finally estimated the tissue regenerative ability of the hydrogels in the rabbit segmental meniscus defect model. The hydrogels were injected into the meniscal regions after 1 week of post-meniscectomy treatment in a minimally invasive way; the animals were sacrificed at 4, 8, and 12 weeks after injection (Figure 6(a)).

The gross observation revealed that the tissues were regenerated in hydrogel-applied groups, whereas the incomplete generation of tissues was shown in the control group (Figure 6(b)). Remarkably, when Fb/F127 and Fb/F127/PMMA were injected, soft tissues started to be formed at 4 weeks; however, native meniscus-like tissues were regenerated over time. More specifically, the tissue surface in the Fb/F127/PMMA group was unevenly formed in some individuals.

The meniscal plate regeneration area at 12 weeks was measured. The Fb/F127 (46.71 ± 14.99 mm^2) and Fb/F127/PMMA (43.83 ± 18.35 mm^2) had significantly higher regenerated area than that of the Fb (13.89 ± 3.64 mm^2) and the control (11.93 ± 4.89 mm^2; Figure 6(c)). We additionally identified the cartilage surface at 12 weeks after the injection of Fb/F127 hydrogel. As a result of the Indian ink staining, we could observe that both the medial femur and tibial surfaces were severely damaged in the control group and also slightly damaged in the Fb group (Figure 7(a)). The histological staining showed a similar result that the damage of the tibial plateau of the control group was remarkably indicated (Figure 7(b)). However, in the case of

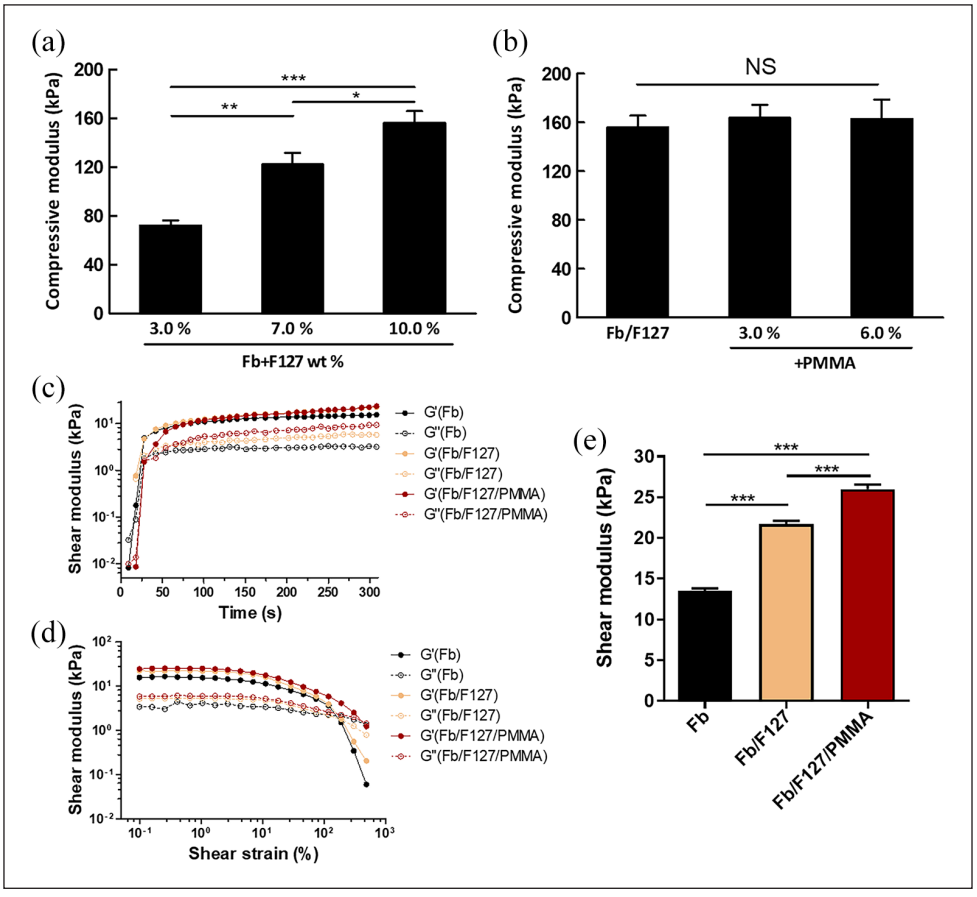

Figure 2. Mechanical properties of the Fb/F127/PMMA hydrogels. The compressive modulus of hydrogels depending on the amount of (a) F127 and (b) PMMA polymers. The incorporation of F127 significantly enhanced the compressive strength, but PMMA did not have much effect on the compression of the hydrogels. (c) The time-dependent viscoelastic behavior of the hydrogels was measured to monitor the gelation time where the storage modulus (G') became over the loss modulus (G'') of hydrogels. The hydrogels could form the gel state within about 50 s. (d) The shear-mediated breakage of the hydrogel was estimated by the strain-sweep mode with the range of strain from 0.1% to 500%. (e) The shear storage modulus of the hydrogels at the equilibrium state and measured in the frequency-sweep mode at 10^2 rad/s of frequency (*$p < 0.05$. **$p < 0.01$. ***$p < 0.001$; $n = 4$–5).

both Fb/F127 and Fb/F127/PMMA, there were few signs of damage to the medial femur tibial surface.

Histological analysis of the regenerated meniscus

The qualitative analysis of the regenerated meniscus was carried out by observing the physiological structure in the histological staining images. In hematoxylin and eosin (H&E) images, the Fb/F127 and Fb/F127/PMMA groups showed an excellent projection of meniscal tissues compared to Fb and control groups (Figure 8(a)). As shown in normal meniscal chondrocytes, the meniscal tissues exist with large circular cells that have round or oval nuclei scattered in the fibrous extracellular matrix, which had been seen to be positively stained with safranin O, type I (COL I), and type II (COL II) collagen. At 4 and 8 weeks, in all groups, cells with a circular nucleus could not be identified, but it was confirmed that a number of small fibrocyte-like cells having a spindle-shaped or rod-like nucleus were penetrated into the defect regions. However, in the Fb/F127 and Fb/F127/PMMA groups at week 12, a large number of cells with a circular nucleus could be observed, whose extracellular matrix were strongly stained with safranin-O (S-O) and collagens; however, the Fb group still represented the cells with spindle-like shapes with relatively less degree of S-O, COL II, and COL I staining. The histological tissue quality score showed that the regenerated meniscus of both Fb/F127 and Fb/F127/PMMA had significant histological differences compared to Fb and control (Figure 8(b)).

In addition, at 12 weeks, the biomechanical property of the meniscal specimens was evaluated using a universal testing machine (Figure 9). The compressive modulus of Fb/F127 and Fb/F127/PMMA groups was 3.50 ± 0.35 and 3.59 ± 0.89 MPa, which were significantly higher than that of other groups (control: 0.23 ± 0.03 MPa; Fb: 0.82 ± 0.05 MPa). Even though the mechanical property

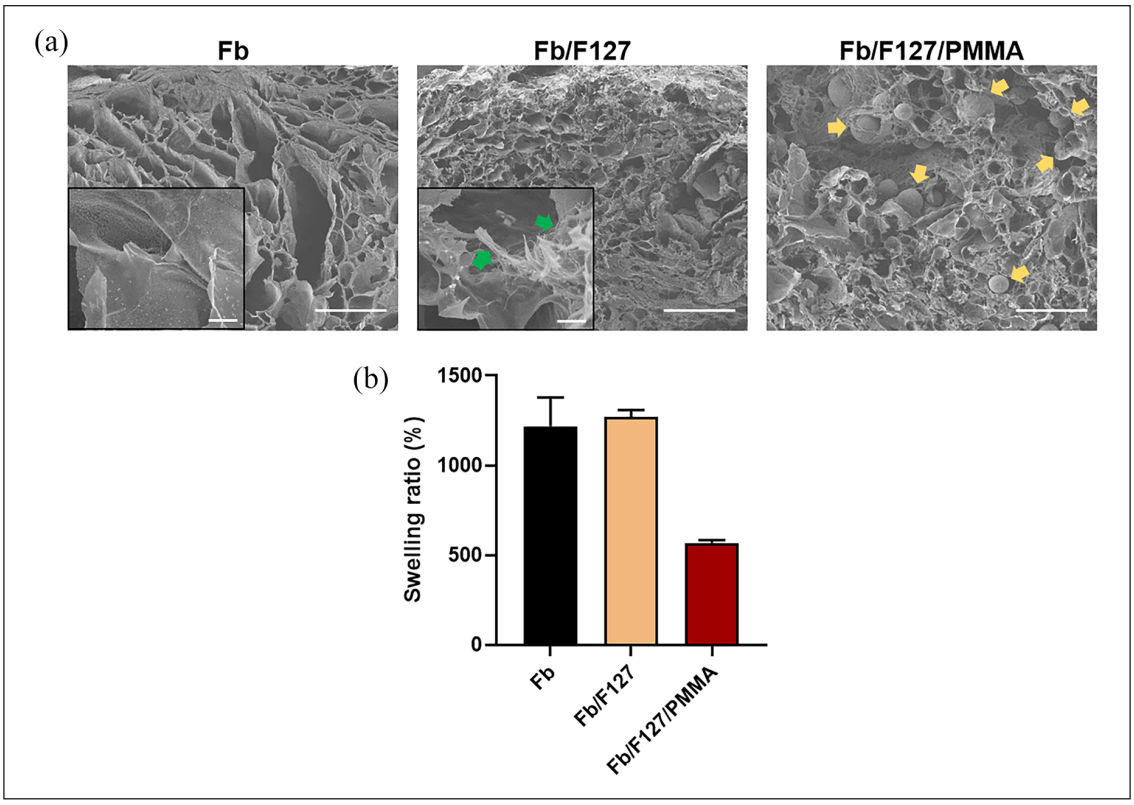

Figure 3. The microstructure and the swelling ratio of hydrogels: (a) SEM images showed the porous structure of the hydrogels. The polymeric branches (green arrow) of F127 were incorporated with the Fb wall in the Fb/F127, and PMMA microbeads (yellow arrow) could be observed in Fb/F127/PMMA (scale bar = 500 μm and scale bar = 10 μm in the inlet images) and (b) the water uptake behavior of both Fb and Fb/F127 was similar to each other; however, that of Fb/F127/PMMA was significantly lowered ($n = 3$).

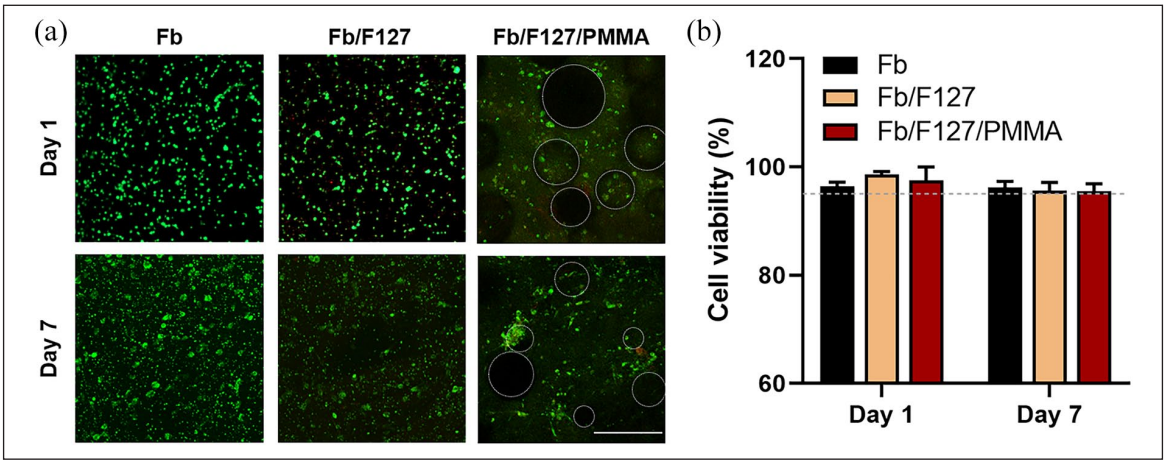

Figure 4. In vitro cytotoxicity test of the hydrogels: (a) The fluorescent images showing live (green) and dead (red) fibrochondrocytes encapsulated in the hydrogels for 7 days (white circle: PMMA microbeads, scale bar = 200 μm) and (b) the cell viability was quantified based on the Live/Dead assay, and it revealed that the cells survived well over 95% of viability ($n = 5–10$).

of the regenerated tissues was inferior to that of normal tissue (6.63 ± 1.12 MPa), it was confirmed that the Fb/F127 and Fb/F127/PMMA groups could recover the segmental defect of the meniscus with enhanced tissue quality.

Discussion

The purpose of this study was to find out the hydrogel-based injectable system that is mechanically stable has improved physiological activity and can be clinically applicable to treat the meniscal defect as translational

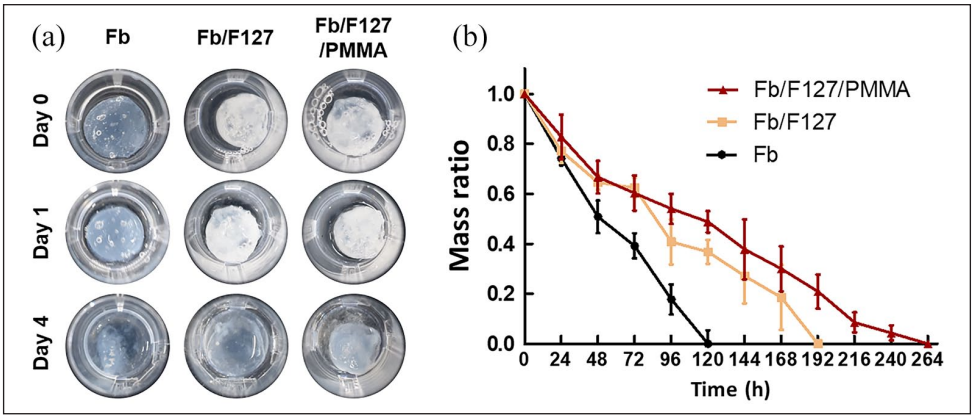

Figure 5. In vitro enzymatic degradation profile of the hydrogels: (a) The hydrogel images showed the trypsin-mediated degradative behavior in vitro and (b) the degradation profile based on the mass ratio demonstrated that both F127 and PMMA polymers could enhance the resistance of hydrogel to enzymatic degradation, indicating that the composite hydrogel had the effect of treating the defect for an extended period ($n = 4–5$).

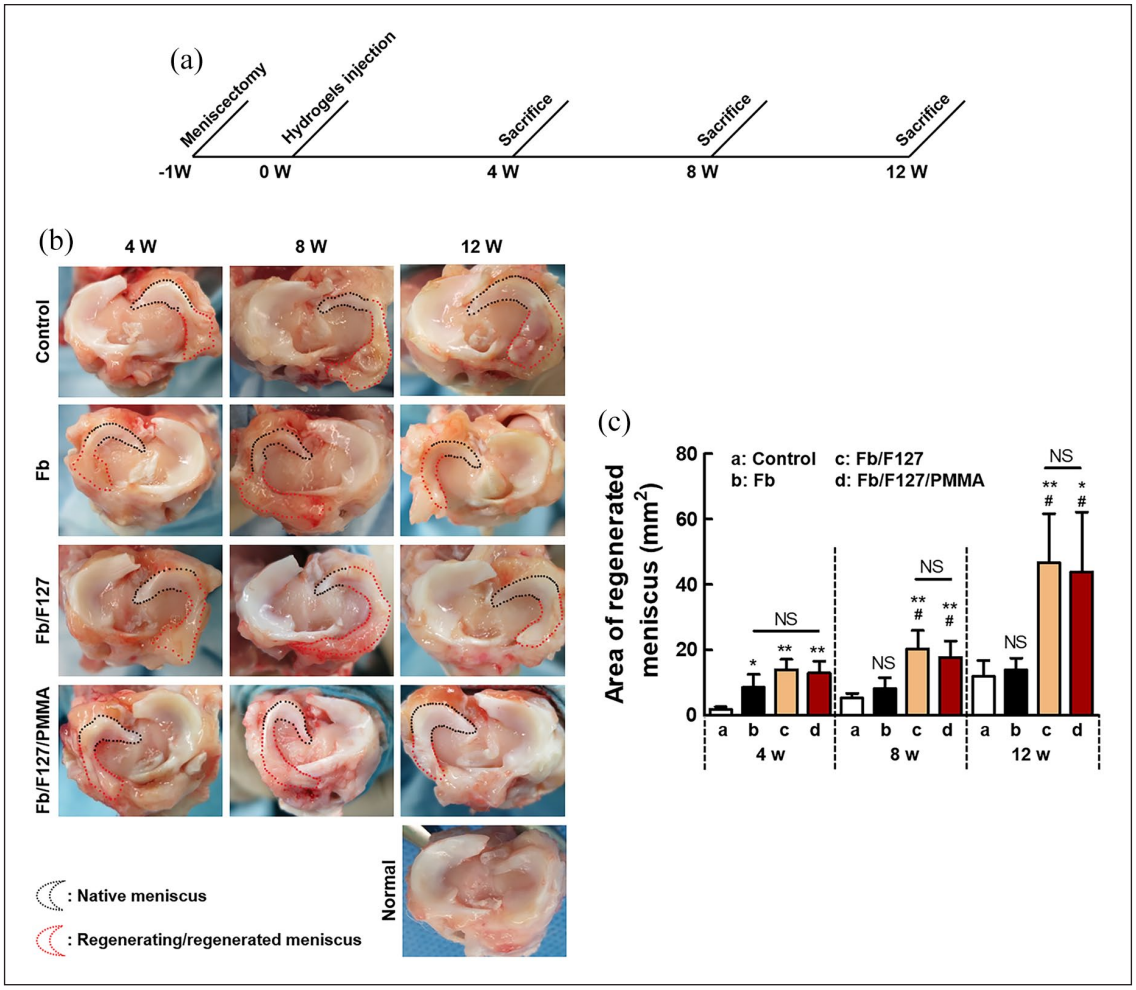

Figure 6. In vivo tissue regenerative ability of hydrogels and macroscopic analysis of the regenerated meniscus after 4, 8, and 12 weeks post-treatment: (a) The schematic diagram for in vivo experiment, (b) gross evaluation of regeneration of rabbit meniscus at 4, 8, and 12 weeks after hydrogel injection, and (c) the quantitative regeneration area was calculated using image-based ImageJ software.

Statistical significance: *Compared to the control group; #Compared to the Fb group; *,#$p < 0.05$. **$p < 0.01$. ***$p < 0.001$.

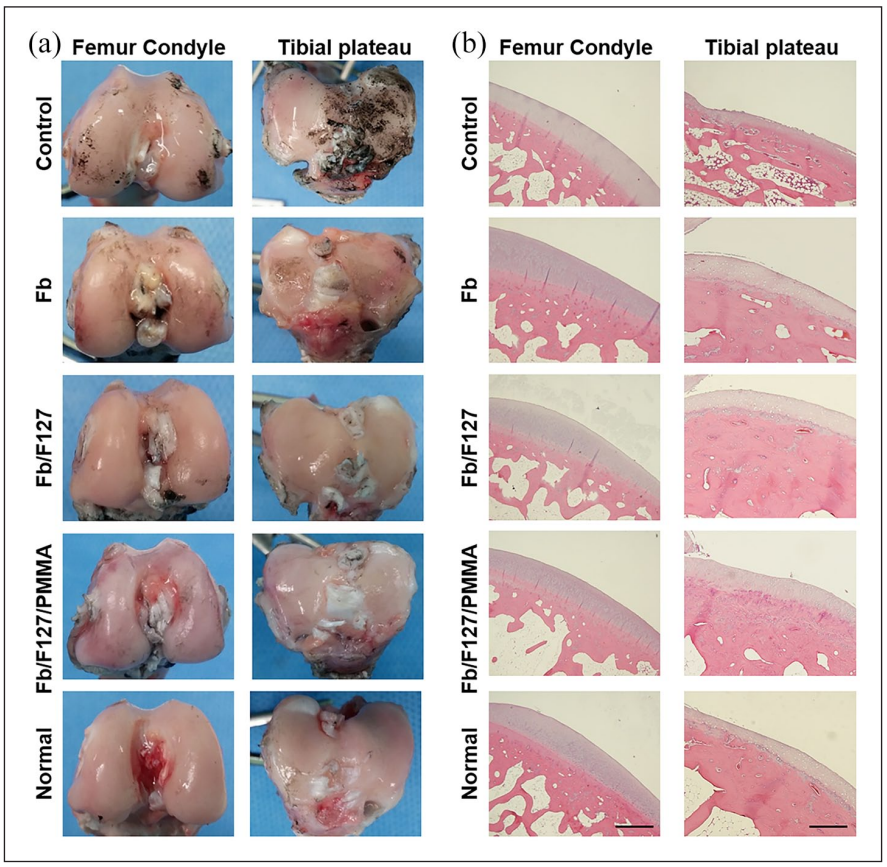

Figure 7. Photograph and histological images of both the femoral condyle and tibial plateau: (a) The cartilage surfaces of both femur condyle and the tibial plateau of each experimental group were treated with the Indian ink staining and (b) the hematoxylin & eosin (H&E) staining images. There was no progressive signal of osteoarthritis in the Fb/F127 and Fb/F127/PMMA groups (scale bar = 200 μm).

research. Fibrin (Fb) is polymerized by the activity of fibrinogen and thrombin, which are bio-derived materials, and is currently used in various biomedical applications as fibrin glue.[23] However, since fibrin is easily decomposed and mechanically unstable in vivo, we herein incorporated synthetic biopolymers into the Fb, that is, Pluronic® F-127 (F127) and poly(methyl methacrylate) (PMMA), which are FDA-approved biomaterials. This injectable hydrogel system can effectively fill the meniscal defect regions; therefore, it is not needed to remove all cartilage plates unnecessarily as in allogeneic meniscal graft transplantation. Moreover, it can shorten the surgery process rather than other biomimetic scaffold-based strategies that required open surgery and suture.

We optimized the concentration of fibrinogen and thrombin to form in situ gelations through the dual-syringe system and here added the synthetic polymers to firstly evaluate the mechanical enhancement of the hydrogel system (Figure 1). The major limitation of the injectable hydrogels is weak mechanical properties, susceptible to load-bearing applications.[43] However, this Fb/F127/PMMA semi-IPN system could withstand the stresses on the surface of knee joints without any damages at the femur condyle and tibial plateau (Figure 7). Once F127 was mixed with Fb, they formed semi-interpenetrated networks (semi-IPN), which significantly enhanced the compressive strength of the hydrogel. Furthermore, PMMA microbeads were dispersed within the hydrogel networks, and it could improve the shear-resistance strength of hydrogels.[44] This Fb-based in situ gelated semi-IPN system has great advantages of using a biological crosslinking mechanism, which is a biocompatible process compared to the potential cytotoxicity of radical polymerization processes.[45,46] It also enables control of the physical and mechanical properties incorporating diverse biomaterials into Fb networks without any chemical modifications. Moreover, the hydrogel had pressure-dependent shape plasticity, which allowed it to tailor its shape to fit the meniscal defect sites. Also, all the materials in this study have been approved to be utilized clinically; therefore, this study is a meaningful achievement of translational research.

We finally confirmed that the incorporation of F127 and PMMA into Fb hydrogel could facilitate the regeneration ability and enhance the quality of the repaired tissue in the in vivo rabbit segmental meniscal defect model. The

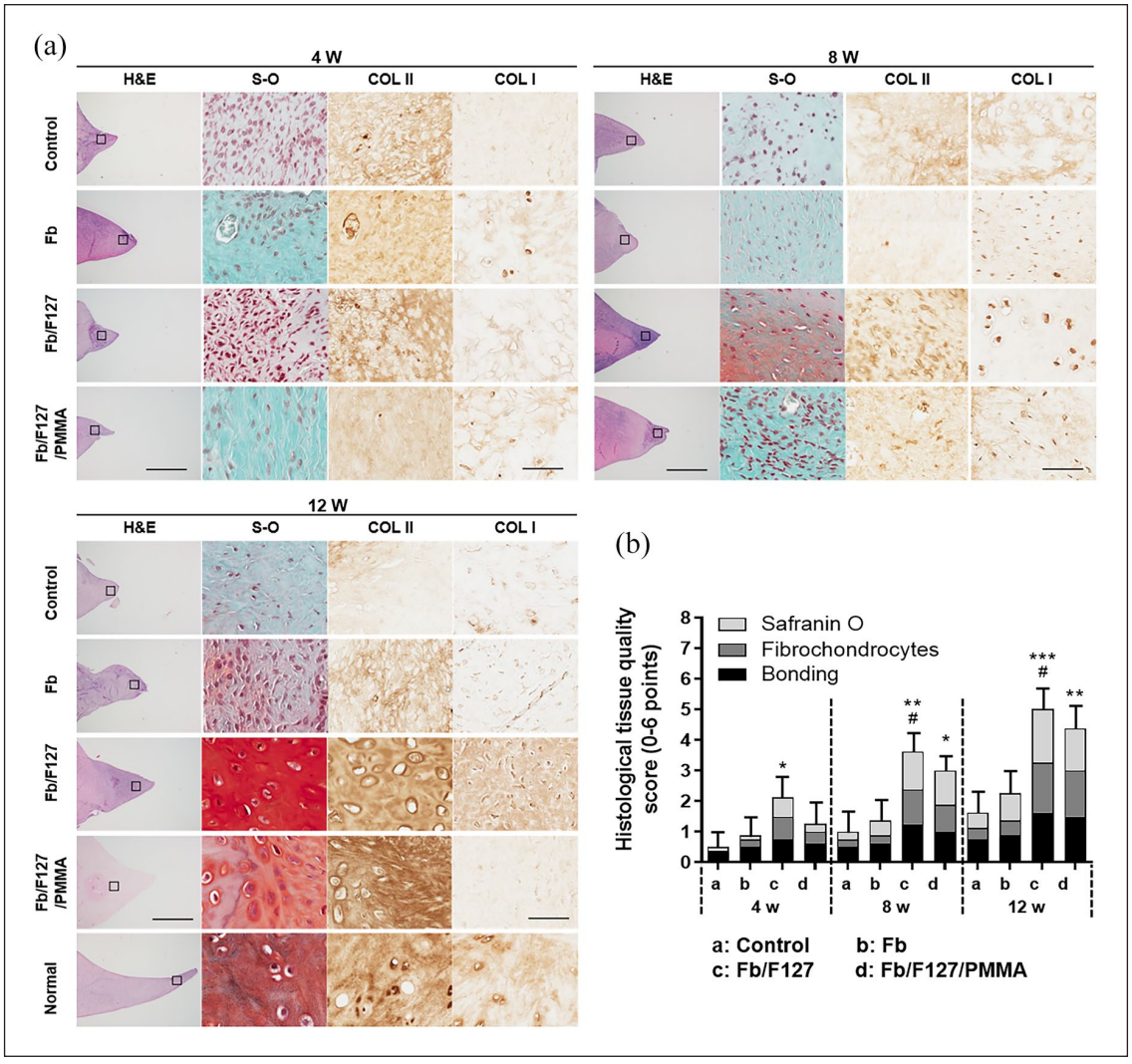

Figure 8. Histological analysis of the regenerated meniscus after hydrogel injection at 4, 8, and 12 weeks: (a) representative sections stained with H&E, safranin-O (S-O), collagen type I and II (COL I and COL II) of the meniscus tissues at 4, 8, and 12 weeks, respectively (scale bar = 2 mm and 100 μm in low and high magnification each) and (b) In vivo semi-quantitative scoring of tissue quality was measured, and each average score was displayed. The total score of Fb/F127 was significantly higher than the other two groups at 8 and 12 weeks.

Statistical significance: *Compared to the control group; #Compared to the Fb group; *,#$p < 0.05$. **$p < 0.01$. ***$p < 0.001$.

high strength of the hydrogel and prolonged degradation time of the Fb/F127/PMMA hydrogel might support both tissue ingrowth and maturation.[47] In the case of Fb/F127, at week 4, lots of rounded cells were gathered as blood vessels were formed in the damaged tissue, and fibroblast-like cells appeared. At 8 weeks, a large number of round cells were seen, and at 12 weeks, fibrocartilage-like cells were also found. When we checked the injected site, the hydrogels were adhered not to the damaged cartilage but to the surrounding connective tissues (data was not shown). This might help the neighbor cells enter and survive better.[17]

Although we did not show the results of regeneration in the early stage, it can be inferred that the regeneration process of the meniscus cartilage was similar to the tissue healing process according to our results (Supplemental Figure 1). In particular, we did not identify the main source of migrating cells, but these cells may be synovial fibroblasts, as the existing literature found extensive synovial proliferation next to the meniscus area.[48,49] In a previous study, the left anterior half of the medial meniscus was resected using C57Bl/6J mice, and the process of meniscal regeneration and cartilage degeneration was investigated.[50] Extensive macrophage infiltration into the synovial membrane around the meniscus site was observed on day 3, and synovial hyperplasia was detected 2 weeks after surgery. At this stage, the synovial tissue was filled with many fibroblastic cells, which underwent chondrocyte differentiation up to 4 weeks after surgery to generate a cartilage matrix. It has also been reported that progenitor cells on

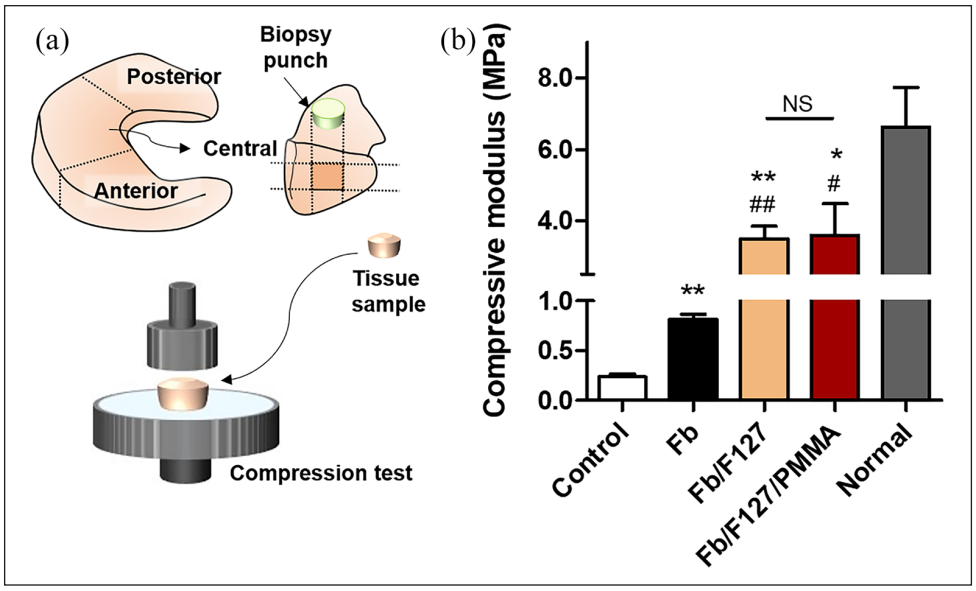

Figure 9. Biomechanical strength of the regenerated meniscal tissue: (a) Schematic illustration for explaining the experimental method. The tissue samples were collected from the central region of the regenerated meniscus at 12 weeks post-treatment, and (b) the compressive modulus of the tissues was measured to analyze the qualitative estimation compared to the normal tissue. Statistical significance: *Compared to the control group; #Compared to the Fb group; $^{*,\#}p < 0.05$ and $^{**,\#\#}p < 0.01$ ($n = 3$).

the meniscus surface migrate from the vascularized red region to the nonvascular white region and participated in the tissue repair,[51] and also that human and rabbit meniscus contain mesenchymal progenitor cells with multiple differentiation capacity.[52–55] Therefore, we believe that the main source of repair cells during meniscus regeneration may be meniscus fibrochondrocytes, synovial fibroblasts, and mesenchymal progenitors present in the outer red or red region.

In addition to this, it has been reported that the vascularity of the damaged area dramatically affects the outcome of meniscus healing.[56] In the inflammatory phase, neutrophil infiltration leads to circulating peripheral blood cells and macrophages. Pro-inflammatory M1 macrophages express CD68, and anti-inflammatory/regenerative M2 macrophages express antigens such as CD163.[57] M1 phagocytosis reveals TNF-α, IL-6, and IL-12 and their cytokines.[58–60] In the proliferative phase, M2 macrophages contribute to tissue healing, angiogenesis, promotion of tumor growth, and immunosuppression.[60] M2 macrophages produce large amounts of IL-10 and TGF-β, promote tissue repair and wound healing, and have angiogenic properties.[61,62] Thus, as in previous studies, it can be inferred that it is derived from various proliferative cytokines derived from M2 macrophages in the inflammatory phase of the meniscus cartilage regeneration mechanism. More details in cellular origins during the initial state of meniscus repair should be further investigated.

The innermost region of the meniscus consists of small, unorganized, radial collagen fibrils with a cartilage-like structure.[63] In the case of cartilage regeneration, lots of studies have mainly used the mesenchymal stem cells (MSCs) or induced cartilage regeneration by treating small molecule drugs, cartilage-inducing factors, and scaffolds together.[64–66] These strategies provide therapeutic efficacy against cartilage damage by activating exogenous MSC differentiation,[66] recruiting endogenous MSCs, or inducing cartilage-associated extracellular matrix formation.[64–66] Even though we used acellular hydrogel, it can be inferred that it would provide therapeutic efficacy for meniscus injury by recruiting endogenous MSCs or surrounding cells or inducing extracellular matrix formation. Due to the complex phenotype and function of meniscus tissue compared to the cartilage tissue,[67] promising results for meniscus therapy are still lacking.[67] The fibrin can provide an inducible extracellular matrix (ECM) to manipulate the regenerative process by promoting migration, proliferation, and differentiation of both macrophages and endogenous stem/progenitor cells, etc.[68] However, in terms of solely use of Fb, it has a fast decomposition rate, so the period of residence of the migrated cells in the damaged area is expected to be short, and it required more time for migrated cells to be differentiated, inferring that the regenerative rate would be delayed with ECM should be newly replenished.

This study has some limitations: the long-term research should be further carried out to evaluate the prolonged effects of hydrogels on tissue repair and the prognosis of the treatment. The regenerated tissues had lower mechanical properties than that of normal menisci (Figure 9); this might be attributed to a reasonably short observation period of 12 weeks. Therefore, it can be possible that

additional tissue maturation may occur with increasing the mechanical properties of tissues. In addition, some biological studies are needed to explore the origin and molecular function of chondrocyte-like cells in regenerated tissue. Finally, the actual load-bearing implication should be further investigated in the large animal model to this injectable semi-IPN hydrogel system would be entered into the clinical trials.

Conclusion

We herein developed an injectable system consist of both natural and synthetic polymers as semi-IPN hydrogel to treat a segmental defect of the meniscus in a rabbit model. The innate weak mechanical properties of fibrin (Fb) could be augmented through adding Pluronic F127 (F127) poloxamer, particularly its shear-resistance capacity enhanced in conjunction with polymethyl methacrylate (PMMA) microbeads. The composite hydrogel also had resistance to enzymatic degradation, which would prolong the therapeutic effects. Finally, in the in vivo rabbit meniscectomy model, the Fb/F127/PMMA hydrogel not only accelerated the tissue regeneration rate but also reconstructed the meniscus with significantly enhanced tissue quality. This highlights that the Fb/F127/PMMA hydrogel would advance the meniscal therapy through a minimally invasive way and had the potential to be used in clinical applications.

Declaration of conflicting interests

The author(s) declared no potential conflicts of interest with respect to the research, authorship, and/or publication of this article.

Funding

The author(s) disclosed receipt of the following financial support for the research, authorship, and/or publication of this article: This work was financially supported by National Research Foundation of Korea (NRF) grants funded by the Ministry of Science and ICT (NRF-2021R1A2C2008821); the K-BIO KIURI Center program (2020M3H1A1073304); the Korea Medical Device Development Fund grant (KMDF_PR_20200901_0151); and the Basic Research Program through the Ministry of Education (2021R1I1A1A01049597). This work was also funded by a grant from the Samsung Medical Center, Republic of Korea (PHX0153801) and the Institute of Engineering Research at Seoul National University provided research facilities for this work.

ORCID iDs

Su-Hwan Kim https://orcid.org/0000-0001-5337-3335
Nathaniel S Hwang https://orcid.org/0000-0003-3735-7727

Supplemental material

Supplemental material for this article is available online.

References

1. Henning CE, Lynch MA and Clark JR. Arthroscopy classics: Vascularity for healing of meniscus repairs. *Arthroscopy* 2010; 26: 1368–1369.
2. De Bruycker M, Verdonk PCM and Verdonk RC. Meniscal allograft transplantation: a meta-analysis. *Sicot J* 2017; 3: 33.
3. Elattar M, Dhollander A, Verdonk R, et al. Twenty-six years of meniscal allograft transplantation: Is it still experimental? A meta-analysis of 44 trials. *Knee Surg Sports Traumatol Arthrosc* 2011; 19: 147–157.
4. Packer JD and Rodeo SA. Meniscal allograft transplantation. *Clin Sports Med* 2009; 28: 259–283, viii.
5. Tienen TG, Heijkants RG, de Groot JH, et al. Replacement of the knee meniscus by a porous polymer implant: a study in dogs.. *Am J Sports Med* 2006; 34: 64–71.
6. Welsing RT, van Tienen TG, Ramrattan N, et al. Effect on tissue differentiation and articular cartilage degradation of a polymer meniscus implant: aa 2-year follow-up study in dogs. *Am J Sports Med* 2008; 36: 1978–1989.
7. Verdonk P, Beaufils P, Bellemans J, et al. Successful treatment of painful irreparable partial meniscal defects with a polyurethane scaffold: two-year safety and clinical outcomes. *Am J Sports Med* 2012; 40: 844–853.
8. Efe T, Getgood A, Schofer MD, et al. The safety and short-term efficacy of a novel polyurethane meniscal scaffold for the treatment of segmental medial meniscus deficiency. *Knee Surg Sports Traumatol Arthrosc* 2012; 20: 1822–1830.
9. Hansen R, Bryk E and Vigorita V. Collagen scaffold meniscus implant integration in a canine model: a histological analysis. *J Orthop Res* 2013; 31: 1914–1919.
10. Kon E, Chiari C, Marcacci M, et al. Tissue engineering for total meniscal substitution: animal study in sheep model. *Tissue Eng Part A* 2008; 14: 1067–1080.
11. Martinek V, Ueblacker P, Bräun K, et al. Second generation of meniscus transplantation: in-vivo study with tissue engineered meniscus replacement. *Arch Orthop Trauma Surg* 2006; 126: 228–234.
12. Zaffagnini S, Marcheggiani Muccioli GM, Lopomo N, et al. Prospective long-term outcomes of the medial collagen meniscus implant versus partial medial meniscectomy: a minimum 10-year follow-up study. *Am J Sports Med* 2011; 39: 977–985.
13. Drobnič M, Ercin E, Gamelas J, et al. Treatment options for the symptomatic post-meniscectomy knee. *Knee Surg Sports Traumatol Arthrosc* 2019; 27: 1817–1824.
14. Dhollander A, Verdonk P and Verdonk R. Treatment of painful, irreparable partial meniscal defects with a polyurethane scaffold: midterm clinical outcomes and survival analysis. *Am J Sports Med* 2016; 44: 2615–2621.
15. Monllau JC, Gelber PE, Abat F, et al. Outcome after partial medial meniscus substitution with the collagen meniscal implant at a minimum of 10 years' follow-up. *Arthroscopy* 2011; 27: 933–943.
16. Lyu Y, Xie J, Liu Y, et al. Injectable hyaluronic acid hydrogel loaded with functionalized human mesenchymal stem cell aggregates for repairing infarcted myocardium. *ACS Biomater Sci Eng* 2020; 6: 6926–6937.

17. Scotti C, Pozzi A, Mangiavini L, et al. Healing of meniscal tissue by cellular fibrin glue: an in vivo study. *Knee Surg Sports Traumatol Arthrosc* 2009; 17: 645–651.
18. Ishimura M, Ohgushi H, Habata T, et al. Arthroscopic meniscal repair using fibrin glue. Part i: experimental study. *Arthroscopy* 1997; 13: 551–557.
19. Hashimoto J, Kurosaka M, Yoshiya S, et al. Meniscal repair using fibrin sealant and endothelial cell growth factor. An experimental study in dogs. *Am J Sports Med* 1992; 20: 537–541.
20. Arnoczky SP, Warren RF and Spivak JM. Meniscal repair using an exogenous fibrin clot: an experimental study in dogs. *J Bone Joint Surg Am* 1988; 70: 1209–1217.
21. Kang SW, Son SM, Lee JS, et al. Regeneration of whole meniscus using meniscal cells and polymer scaffolds in a rabbit total meniscectomy model. *J Biomed Mater Res* 2006; 78A: 638–651.
22. Ishida K, Kuroda R, Miwa M, et al. The regenerative effects of platelet-rich plasma on meniscal cells in vitro and its in vivo application with biodegradable gelatin hydrogel. *Tissue Eng* 2007; 13: 1103–1112.
23. Roberts IV, Bukhary D, Valdivieso CYL, et al. Fibrin matrices as (injectable) biomaterials: formation, clinical use, and molecular engineering. *Macromol Biosci* 2020; 20: e1900283.
24. Kim JA, An YH, Yim HG, et al. Injectable fibrin/polyethylene oxide semi-IPN hydrogel for a segmental meniscal defect regeneration. *Am J Sports Med* 2021; 49: 1538–1550.
25. Lee F and Kurisawa M. Formation and stability of interpenetrating polymer network hydrogels consisting of fibrin and hyaluronic acid for tissue engineering. *Acta Biomater* 2013; 9: 5143–5152.
26. Hwang CM, Ay B, Kaplan DL, et al. Assessments of injectable alginate particle-embedded fibrin hydrogels for soft tissue reconstruction. *Biomed Mater* 2013; 8: 014105.
27. Quintans-Júnior LJ, Brito RG, Quintans JSS, et al. Nanoemulsion thermoreversible Pluronic F127-based hydrogel containing hyptis pectinata (lamiaceae) leaf essential oil produced a lasting anti-hyperalgesic effect in chronic noninflammatory widespread pain in mice. *Mol Neurobiol* 2018; 55: 1665–1675.
28. Nie S, Hsiao WL, Pan W, et al. Thermoreversible Pluronic F127-based hydrogel containing liposomes for the controlled delivery of paclitaxel: in vitro drug release, cell cytotoxicity, and uptake studies.. *Int J Nanomedicine* 2011; 6: 151–166.
29. Shimizu Y, Sakakibara K, Akimoto S, et al. Effective reinforcement of poly(methyl methacrylate) composites with a well-defined bacterial cellulose nanofiber network. *ACS Sustain Chem Eng* 2019; 7: 13351–13358.
30. Guvendiren M, Messersmith PB and Shull KR. Self-assembly and adhesion of dopa-modified methacrylic triblock hydrogels. *Biomacromolecules* 2008; 9: 122–128.
31. Guvendiren M and Shull KR. Self-assembly of acrylic triblock hydrogels by vapor-phase solvent exchange. *Soft Matter* 2007; 3: 619–626.
32. Mueller SM, Shortkroff S, Schneider TO, et al. Meniscus cells seeded in type I and type II collagen-gag matrices in vitro. *Biomaterials* 1999; 20: 701–709.
33. Shen W, Chen J, Zhu T, et al. Osteoarthritis prevention through meniscal regeneration induced by intra-articular injection of meniscus stem cells. *Stem Cells Dev* 2013; 22: 2071–2082.
34. Horie M, Sekiya I, Muneta T, et al. Intra-articular injected synovial stem cells differentiate into meniscal cells directly and promote meniscal regeneration without mobilization to distant organs in rat massive meniscal defect. *Stem Cells* 2009; 27: 878–887.
35. Kobayashi K, Amiel M, Harwood FL, et al. The long-term effects of hyaluronan during development of osteoarthritis following partial meniscectomy in a rabbit model. *Osteoarthr Cartil* 2000; 8: 359–365.
36. Visco DM, Hill MA, Widmer WR, et al. Experimental osteoarthritis in dogs: a comparison of the pond-nuki and medial arthrotomy methods. *Osteoarthr Cartil* 1996; 4: 9–22.
37. Katagiri H, Muneta T, Tsuji K, et al. Transplantation of aggregates of synovial mesenchymal stem cells regenerates meniscus more effectively in a rat massive meniscal defect. *Biochem Biophys Res Commun* 2013; 435: 603–609.
38. Park YB, Ha CW, Kim JA, et al. Effect of transplanting various concentrations of a composite of human umbilical cord blood-derived mesenchymal stem cells and hyaluronic acid hydrogel on articular cartilage repair in a rabbit model. *PLoS One* 2016; 11: e0165446.
39. Horie M, Driscoll MD, Sampson HW, et al. Implantation of allogenic synovial stem cells promotes meniscal regeneration in a rabbit meniscal defect model. *J Bone Joint Surg Am* 2012; 94: 701–712.
40. Driscoll MD, Robin BN, Horie M, et al. Marrow stimulation improves meniscal healing at early endpoints in a rabbit meniscal injury model. *Arthroscopy* 2013; 29: 113–121.
41. Gsib O, Duval JL, Goczkowski M, et al. Evaluation of fibrin-based interpenetrating polymer networks as potential biomaterials for tissue engineering. *Nanomater* 2017; 7: 436–456.
42. Shin H, Jo S and Mikos AG. Biomimetic materials for tissue engineering. *Biomaterials* 2003; 24: 4353–4364.
43. Kaya G and Oytun F. Rheological properties of injectable hyaluronic acid hydrogels for soft tissue engineering applications. *Biointerface Res Appl Chem* 2020; 11: 8424–8430.
44. Jiang W, Sun Y, Xu Y, et al. Shear-thickening behavior of polymethylmethacrylate particles suspensions in glycerine–water mixtures. *Rheologica Acta* 2010; 49: 1157–1163.
45. Mironi-Harpaz I, Wang DY, Venkatraman S, et al. Photopolymerization of cell-encapsulating hydrogels: crosslinking efficiency versus cytotoxicity. *Acta Biomater* 2012; 8: 1838–1848.
46. Temenoff JS, Shin H, Conway DE, et al. In vitro cytotoxicity of redox radical initiators for cross-linking of oligo(poly(ethylene glycol) fumarate) macromers. *Biomacromolecules* 2003; 4: 1605–1613.
47. Baek J, Chen X, Sovani S, et al. Meniscus tissue engineering using a novel combination of electrospun scaffolds and human meniscus cells embedded within an extracellular matrix hydrogel. *J Orthop Res* 2015; 33: 572–583.
48. Hatsushika D, Muneta T, Horie M, et al. Intraarticular injection of synovial stem cells promotes meniscal regeneration in a rabbit massive meniscal defect model. *J Orthop Res* 2013; 31: 1354–1359.

49. Nakagawa Y, Muneta T, Kondo S, et al. Synovial mesenchymal stem cells promote healing after meniscal repair in microminipigs. *Osteoarthr Cartil* 2015; 23: 1007–1017.
50. Hiyama K, Muneta T, Koga H, et al. Meniscal regeneration after resection of the anterior half of the medial meniscus in mice. *J Orthop Res* 2017; 35: 1958–1965.
51. Seol D, Zhou C, Brouillette MJ, et al. Characteristics of meniscus progenitor cells migrated from injured meniscus. *J Orthop Res* 2017; 35: 1966–1972.
52. Gui J, Zhang J and Huang H. Isolation and characterization of meniscus derived stem cells from rabbit as a possible treatment for damages meniscus. *Curr Stem Cell Res Ther* 2015; 10: 353–363.
53. Huang H, Wang S, Gui J, et al. A study to identify and characterize the stem/progenitor cell in rabbit meniscus. *Cytotechnology* 2016; 68: 2083–2103.
54. Segawa Y, Muneta T, Makino H, et al. Mesenchymal stem cells derived from synovium, meniscus, anterior cruciate ligament, and articular chondrocytes share similar gene expression profiles. *J Orthop Res* 2009; 27: 435–441.
55. Shen W, Chen J, Zhu T, et al. Intra-articular injection of human meniscus stem/progenitor cells promotes meniscus regeneration and ameliorates osteoarthritis through stromal cell-derived factor-1/CXCR4-mediated homing. *Stem Cells Transl Med* 2014; 3: 387–394.
56. Arnoczky SP and Warren RF. Microvasculature of the human meniscus. *Am J Sports Med* 1982; 10: 90–95.
57. Snelgrove SL, Kausman JY, Lo C, et al. Renal dendritic cells adopt a pro-inflammatory phenotype in obstructive uropathy to activate t cells but do not directly contribute to fibrosis. *Am J Pathol* 2012; 180: 91–103.
58. Gordon S. Alternative activation of macrophages. *Nat Rev Immunol* 2003; 3: 23–35.
59. Mantovani A, Sica A, Sozzani S, et al. The chemokine system in diverse forms of macrophage activation and polarization. *Trends Immunol* 2004; 25: 677–686.
60. Sica A and Mantovani A. Macrophage plasticity and polarization: in vivo veritas. *J Clin Investig* 2012; 122: 787–795.
61. Martinez FO, Sica A, Mantovani A, et al. Macrophage activation and polarization. *Front Biosci* 2008; 13: 453–461.
62. Zizzo G, Hilliard BA, Monestier M, et al. Efficient clearance of early apoptotic cells by human macrophages requires M2c polarization and MerTK induction. *J Immunol* 2012; 189: 3508–3520.
63. Andrews SH, Ronsky JL, Rattner JB, et al. An evaluation of meniscal collagenous structure using optical projection tomography. *BMC Med Imaging* 2013; 13: 21.
64. Chen MJ, Whiteley JP, Please CP, et al. Identifying chondrogenesis strategies for tissue engineering of articular cartilage. *J Tissue Eng* 2019; 10: 2041731419842431.
65. Le H, Xu W, Zhuang X, et al. Mesenchymal stem cells for cartilage regeneration. *J Tissue Eng* 2020; 11: 2041731420943839.
66. Voga M, Drnovsek N, Novak S, et al. Silk fibroin induces chondrogenic differentiation of canine adipose-derived multipotent mesenchymal stromal cells/mesenchymal stem cells. *J Tissue Eng* 2019; 10: 2041731419835056.
67. Jacob G, Shimomura K, Krych AJ, et al. The meniscus tear: a review of stem cell therapies. *Cells* 2019; 9: 92–108.
68. Li H, Yang Z, Fu L, et al. Advanced polymer-based drug delivery strategies for meniscal regeneration. *Tissue Eng Part B Rev* 2021; 27: 266–293.